Grasp Planning with a Soft Reconfigurable Gripper Exploiting Embedded and Environmental Constraints

(Article begins on next page)

Grasp planning with a soft reconfigurable gripper exploiting embedded and environmental constraints

Enrico Turco[1,2], Valerio Bo[1,3], Maria Pozzi[1,3], Alessandro Rizzo[4] and Domenico Prattichizzo[1,3]

Abstract—**Grasping in unstructured environments requires highly adaptable and versatile hands together with strategies to exploit their features to get robust grasps. This paper presents a method to grasp objects using a novel reconfigurable soft gripper with embodied constraints, the Soft ScoopGripper (SSG). The considered grasp strategy, called *scoop grasp*, exploits the SSG features to perform robust grasps. The embodied constraint, i.e., a scoop, is used to slide between the object and a flat surface (e.g., table, wall) in contact with it. The fingers are first configured according to the object geometry and then used to establish reliable contacts with it. This work introduces an algorithm that, given the object point cloud, computes the best pre-grasp gripper configuration from which to start the scoop grasp strategy. Several experimental trials in different scenarios confirmed the effectiveness of the proposed method.**

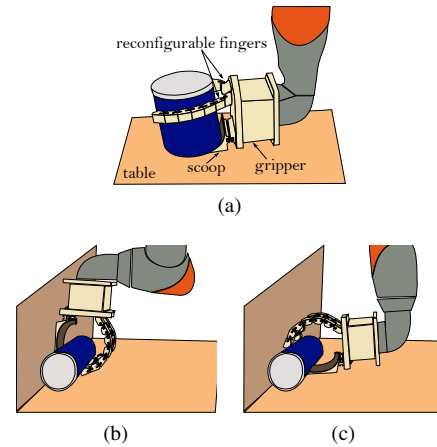*Index Terms*—**Soft Robot Applications; Underactuated Robots; Grasping.**

Fig. 1: Scoop grasp: a soft gripper uses an embedded constraint (scoop) to slide over an environmental constraint (table or wall) and reach the object. Then, reconfigurable soft fingers grasp it.

I. INTRODUCTION

Recent studies showed that in grasping tasks, mainly when there are uncertainties in the object pose, humans tend to exploit environmental features to pick objects up [1]. This is possible thanks to the adaptability and compliance of human hands, and can be replicated with robots exhibiting active or passive compliant behaviors [2]. Bimbo et al. [3] and Hang et al. [4], for example, proposed different ways to implement the so-called *slide-to-edge grasp*, in which an object is dragged towards the edge of a table and then grasped from the side.

Salvietti et al., in [5], introduced a different point of view, embedding a constraint directly in the robotic hand. They presented the Soft ScoopGripper (SSG), a novel hand composed of two soft modular fingers and a tendon-driven scoop connected through a flexible hinge to the hand palm. Acting on the dovetail joints at the bases of the fingers, it is possible to obtain several hand configurations. While in [5] this motion was obtained manually, here we adopt a new version of the SSG, where each finger can be automatically rotated

[1]Istituto Italiano di Tecnologia, Genoa, Italy {enrico.turco, valerio.bo}@iit.it

[2]Dept. of Information Engineering, University of Pisa, Italy.

[3]Dept. of Information Engineering and Mathematics, University of Siena, Italy {maria.pozzi, domenico.prattichizzo}@unisi.it

[4]Dept. of Electronics and Telecommunications, Politecnico di Torino, Italy. {alessandro.rizzo}@polito.it

Digital Object Identifier (DOI): see top of this page.

of an arbitrary angle about its axis. A sketch of the hand is depicted in Fig. 1.

In this paper, we propose a method to plan grasps with the Soft ScoopGripper explicitly taking into account and exploiting its features. The considered grasp strategy is the so-called *scoop grasp* (Fig. 1), where the scoop adapts its orientation to the surface where it slides (e.g., table or wall), while the soft fingers establish reliable contacts with the object and cage it over the scoop. Two main situations are considered: *i)* the object to be grasped is in contact with only one environmental constraint (e.g., table, Fig. 1a), and *ii)* the object touches two different surfaces (e.g., wall and table, Figs. 1b-c).

The grasps depicted in Fig. 1 take inspiration from the so-called *surface-constrained grasp* and *slide-to-wall grasp* [1]. In [1], however, the two strategies are performed by a multi-fingered soft hand and require two very different motions. A scoop grasp, instead, can be performed on surfaces with different inclinations without substantially modifying the adopted strategy. This is possible because the exploitation of environmental features is facilitated by the presence of the actuated scoop, which offers an additional embedded constraint besides the palm.

Indeed, similarly to [6] and [1], the passive compliance of the SSG allows shape adaptation between hand, object, and environment, and further improves grasp success. While there are works that consider completely rigid embedded constraints [7], passive adaptability in the gripper structure was found to be very important in other works presenting a

"scooping grasp" strategy [8].

In this paper, we extend the concept of scooping grasps to include cases in which objects are constrained from two sides and the scoop can either slide on horizontal surfaces, or on vertical ones. This level of flexibility is obtained thanks to a grasp planning algorithm that, based on the point cloud of the object, computes the desired pre-grasp configuration of the hand with respect to the object, rather than the exact position of contact points as done in [8].

In our method, pre-grasp parameters are computed by solving an optimization problem in simulation, then the real SSG is configured accordingly, and the hand-environment-object interaction is exploited to achieve the grasp. In this way, we leave the grasp execution to the gripper "intelligence", without attempting to exactly control the unpredictable interplay between hand, environment, and object. This principle is at the basis of recent methods for planning grasps with soft and underactuated robotic hands. Thanks to the presence of passive compliance in their mechanical structures, these devices are adaptable, versatile, and robust. Thus, we can say that part of the "intelligence" of the grasping system is already embodied in the hardware design, and it is not all demanded to the planning and control algorithms. In light of this, classical grasp planning methods, prescribing the exact position of fingers for ensuring force closure, need to be extended, or even overcome, to exploit the intrinsic features of soft hands [2]. In [3], [9], for example, soft robotic hands are pre-shaped and suitably aligned over the object to obtain edge-grasps and top-grasps, respectively. In other works, human demonstrations were used to define motion primitives [10] or pre-grasp hand orientations [11] for a soft anthropomorphic hand. In [12], a Convolutional Neural Network is used to estimate suitable grasp poses and wrist orientations for a soft gripper.

Previously cited papers present model- and learning-based methods to achieve pre-grasp configurations or perform motion primitives that, combined with the hand adaptability, allow to achieve successful grasps. In this paper, we build on a similar principle, but we propose an algorithm that is suitable for hands with embedded constraints, like the SSG.

The paper is organized as follows. The grasp planning algorithm is introduced in Sec. II, and its experimental validation through multiple grasping trials is presented in Sec. III. The discussion of the results is included in Sec. IV, and the conclusions of the paper are outlined in Sec. V.

II. METHODOLOGY

A. The Soft ScoopGripper

The Soft ScoopGripper (SSG) is a non-anthropomorphic underactuated robotic gripper composed of two soft fingers and a flat surface connected through a flexible hinge to the hand palm (the "scoop"). The fingers can be simultaneously flexed thanks to a tendon-driven differential system actuated by one motor. The scoop can be closed towards the fingers through a tendon-driven mechanism actuated by another motor. The new version of the gripper used in this paper has two additional degrees of actuation that allow to rotate the dovetail joints placed at fingers' bases up to $180°$. Several types

of passively compliant grippers have been proposed in the literature, from tendon-driven structures [13], to completely soft devices [14]. In the first, modules made of soft and rigid materials are usually combined to achieve a trade-off between compliance and grasp strength [15]. In the second, bio-inspired elements, such as spring reinforced [16] or spine-inspired [17] actuators, can be employed to guarantee a satisfactory dynamic performance of the gripper. The SSG falls in the first category of soft grippers as it has modular rigid links connected by flexible joints.

Similarly to multimodal grippers, the SSG can be reconfigured according to the object to grasp. However, in the SSG, the performed grasp is always the result of an enveloping movement (i.e., the fingers close towards each other, as in Fig. 1a, or both against the scoop, as in Figs. 1b-c), while, in multimodal grippers, different grasping modes, not necessarily based on closing motions (e.g., suction cups [18]), can be combined.

B. Optimization problem

In this paper, we present a method to choose the pre-grasp pose of the SSG based on an optimization algorithm. The vector $\mathbf{x}$ of decision variables contains the angles of the dovetail joints θ_R and θ_L, the distance between object and scoop centers d, the orientation of the scoop γ with respect to the object, and the inclination of the gripper α (see Fig. 2):

$$\mathbf{x} = [\theta_R, \theta_L, d, \gamma, \alpha]. \tag{1}$$

The values of γ vary in an interval whose end points depend on the portion of workspace that is reachable by the robot for a certain object pose.

The optimization problem is formulated as follows:

$$\underset{\mathbf{x}}{\text{maximize}} \quad GQI(\mathbf{x}) + \frac{A_{scoop}(\mathbf{x})}{A_{tot}}. \tag{2}$$

The main components of the cost function are a grasp quality index and the ratio between the area of the scoop occupied by the object (A_{scoop}) and the total area of the scoop (A_{tot}). In our simulations and experiments, we chose the Grasp Isotropy Index (GII)[1] [20] as grasp quality index. In principle, however, it is possible to choose any other metric that can be computed based on the knowledge of the quasi-static model of the grasp [19]. The only precaution to be taken consists in the normalization of the index. The second term of the cost function is meant to give more importance to the solutions which maximize the use of the embodied constraint. An analysis of its role is presented at the end of this section. Given that both the terms vary between 0 and 1, the value of the cost function varies in the interval $[0, 2]$. The closer is the value to 2, the better is the solution.

Our problem is non-convex and as solver we adopted a genetic algorithm [21]. We generated an initial population

---

[1]The GII is the ratio between the minimum and the maximum singular values of the Grasp Matrix $\mathbf{G}$: $GII = \sigma_{min}(\mathbf{G})/\sigma_{max}(\mathbf{G})$. This index approaches 1 when the grasp is isotropic (optimal case), and falls to zero when the grasp is close to a singular configuration. For more details on the computation of the Grasp Matrix the reader can refer to [19].
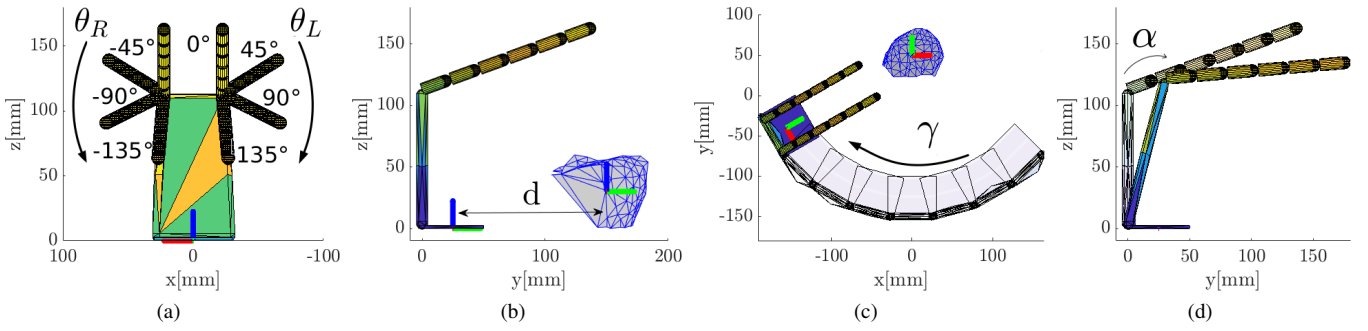
Fig. 2: Decision variables of the optimization problem in Eq. (2): a) θ_R and θ_L express rotations of right and left dovetail joints, respectively. Joint axes point towards the palm of the hand; b) d is the distance between the object center and the scoop center; c) γ represents a rotation referred to the scoop frame around the *z-axis* of the object reference frame; d) α represents a rotation referred to the scoop frame around its *x-axis*. The axes are represented in red (x), green (y), and blue (z).

of 50 individuals where the genes represent our constrained variables in (1). We adopted (2) as a fitness function. The best individuals were chosen using the Tournament Selection to speed up the entire process. After each generation, we generated the children with a scattered crossover function, such that the variables are inherited by the new individuals with a random binary vector. We adopted an adaptive mutation algorithm that randomly generates adaptive directions for the last successful or unsuccessful generation. The algorithm stops when the average relative change in the fitness function value is less than a certain threshold δ. We assumed $\delta = 0.05$. We noticed that, in the worst case, the algorithm stops after the 10th generation.

The grasp simulations needed to solve the optimization problem were carried out using the SynGrasp MATLAB Toolbox [22], in which we defined the model of the SSG depicted in Fig. 2. The optimization algorithm takes as input the normal to the plane on which the scoop should slide and the point cloud of the object to be grasped. Then, the hand model is rotated in the frame of the selected plane and for each combination of decision variables selected by the solver, a grasp is generated by closing the simulated SSG over the model of the object obtained from the point cloud. To compute the contact points necessary to evaluate the GII, we developed a contact detection algorithm implemented in SynGrasp that progressively closes the hand over the object, and geometrically finds the final contact points. More details on scene segmentation and grasp execution are in Sec. II-C.

To better characterize the contribution of the second term in (2), we analysed the results of the optimization carried out with two different objective functions:

$$f_{o1} = GII(\mathbf{x}), \quad f_{o2} = GII(\mathbf{x}) + \frac{A_{scoop}(\mathbf{x})}{A_{tot}}.$$

We acquired the point cloud of 11 different objects (see Table II). We ran the optimization algorithm five times for each objective function, and for each object, considering the object always in the same pose. We noticed that the presence of the second term remarkably affects the solutions found for the distance d between scoop and object centers. Obtained results are reported in Table I and show that both the mean values and the standard deviations of the distance d are lower

TABLE I: Optimization results for the variable d averaged over 5 trials for each condition.

Object	Obj. fct.	d (mm)	Object	Obj. fct.	d (mm)
apple	f_{o1}	28.2($\pm$4.26)	banana	f_{o1}	8.45($\pm$10.7)
	f_{o2}	9.39($\pm$1.45)		f_{o2}	0.47($\pm$1.82)
bowl	f_{o1}	11.1($\pm$15.1)	chips	f_{o1}	26.4($\pm$10.7)
	f_{o2}	0.22($\pm$2.37)	can	f_{o2}	21.2($\pm$0.89)
spring	f_{o1}	3.59($\pm$7.03)	plastic	f_{o1}	20.5($\pm$8.93)
clamp	f_{o2}	0.53($\pm$0.92)	funnel	f_{o2}	4.57($\pm$0.91)
gelatin	f_{o1}	11.2($\pm$8.11)	mug	f_{o1}	24.9($\pm$13.5)
box	f_{o2}	0.8($\pm$0.51)		f_{o2}	12.3($\pm$5.27)
pasta	f_{o1}	18.9($\pm$8.72)	screw-	f_{o1}	4.74($\pm$1.83)
pack	f_{o2}	9.49($\pm$3.56)	driver	f_{o2}	1.36($\pm$0.73)
toy	f_{o1}	3.39($\pm$1.66)			
dolphin	f_{o2}	1.67($\pm$0.83)			

when the second term is present. A lower average distance translates into a pre-grasp pose in which the gripper is closer to the object, and thus the scoop is exploited more. Lower standard deviations, instead, indicate that f_{o2} gives more repeatable and reliable solutions, increasing the robustness of the algorithm [23]. Using the optimization results reported in Table I, we made a short comparison between f_{o1} and f_{o2} in terms of grasp success rate in real experiments. We chose 3 objects in the dataset (apple, chips can, box) and performed 5 trials per object, per function. The success rate obtained when using f_{o2} (93%, 14 out of 15) is remarkably higher with respect to that achieved with f_{o1} (60%, 9 out of 15).

C. Scene segmentation and grasp execution

We adopted the Object Recognition Kitchen Tabletop pipeline [24], to recognize the planes that are present in the scene (captured through an RGB-D camera), and identify a cluster of 3D points belonging to the object. The extraction of the cluster is performed using the Point Cloud Library (PCL) [25], that allows to process the point cloud coming from the camera. The point cloud of the object is then opportunely processed using the Crust algorithm to reconstruct the object shape [26].
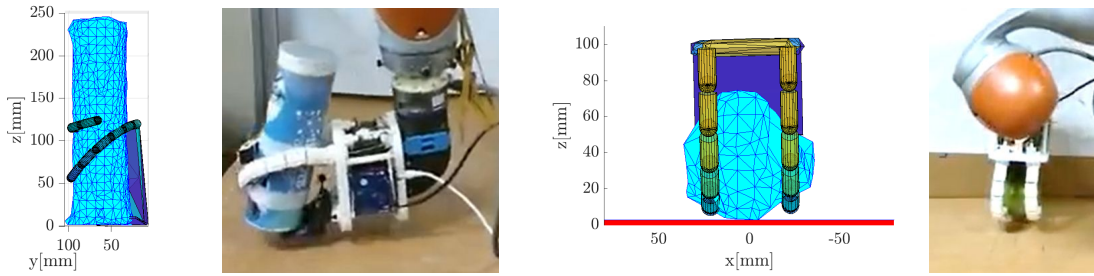
Fig. 3: Simulated result of the optimization and corresponding real experimental trial for a cylindrical object (chips can) grasped from the table (left), and for a spherical object (apple) grasped by sliding the gripper over a vertical wall (right).

Once the main features of the scene are correctly detected and the sliding plane is selected, the grasp planning algorithm based on the optimization problem in Eq. (2) can start searching for the optimal pre-grasp pose, that we indicate with $\mathbf{x}^* = [\theta_R^*, \theta_L^*, d^*, \gamma^*, \alpha^*]$.

Based on the result of the optimization, the execution of the grasp proceeds as follows. The orientation of the fingers is set using the two servo motors to achieve θ_R^* and θ_L^*. Then, the robot arm supporting the SSG is moved to let the scoop rotate of an angle γ^*. Hence, a hybrid force-velocity controller is implemented such that the SSG moves towards the surface to slide on until it touches the surface itself. Upon termination, the scoop is moved towards the object at a constant speed $\vec{v}$ parallel to the surface, while maintaining a constant force in the direction normal to the surface. During its sliding motion towards the object, the end-effector is rotated with respect to the table surface by an angle α^*. Thus, the angular velocity of the robot end-effector is computed as: $\vec{\omega}(t) = (\vec{v}(t)/d(t)) \cdot \alpha^*$, where $d(t)$ is the distance between the object and the hand. Once the distance between the hand and the object reaches the desired value d^*, the gripper controller flexes the fingers until they touch the object. Then, the scoop is actuated, and the object is pushed against the palm until it is caged.

Two examples of the simulated outcomes of the optimization and their real counterparts are shown in Fig. 3. While the cylindrical chips can is grasped from the table, the apple is grasped sliding the scoop over the wall.

III. EXPERIMENTAL RESULTS

The experimental setup, shown in Fig. 4, included a LBR iiwa 7 robot arm (KUKA AG), a Gamma 6-axis force-torque sensor (ATI Industrial Automation, Inc.), and the Soft ScoopGripper attached to the end-effector [5]. A Kinect One RGB-D camera (Microsoft) was used to detect objects and planes in the scene as described in Sec. II-C.

The adopted dataset of objects is shown in Fig. 4 and described in Table II. The objects were chosen to have a wide range of sizes, weights and shapes and most of them come from the YCB Dataset [27]. The apple, the gelatin box, and the chips have paradigmatic shapes (sphere, cuboid, cylinder); the banana, the spring clamp, and the screwdriver have a small height and diverse shapes; the pasta pack is heavy; the toy dolphin is deformable; the funnel has a complex shape and can rotate when touched; the mug and the bowl are hollow.
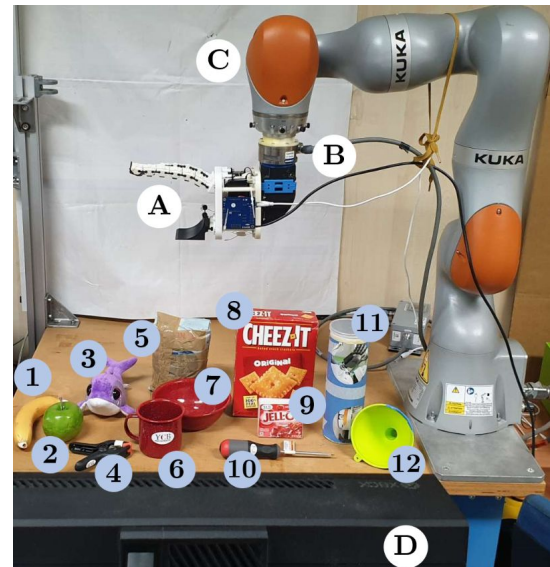

Fig. 4: Experimental setup and dataset of objects. (A) Soft ScoopGripper, (B) ATI F/T sensor, (C) KUKA LBR iiwa, and (D) Kinect. Objects are indicated with numerical IDs and their properties are reported in Table II.

The cracker box was only used in Experiment 3 as a support for another object.

Three experiments were performed to test the grasp planning algorithm explained in Sec. II. Experiment 1 was meant to test the effectiveness of the grasp planner when dealing with objects in contact with just one surface in the environment, i.e., laying on a table. In this case, the success rate over 11 different objects, picked up 10 times each, was evaluated in correlation to objects' characteristics. Experiment 2 aimed at testing the scoop grasp in situations in which the object is in contact with two different surfaces, i.e., table and wall. Here, the most relevant aspect to study was where to slide the scoop to obtain higher success rates, given objects' features. Experiment 3 had the objective of showing the applicability of the proposed grasping strategies in real world scenarios, including grasping in clutter or inside boxes. In all the experiments, a grasp was considered successful if the object was picked up and moved to the final position without falling. Otherwise, it was considered unsuccessful.

This article has been accepted for publication in a future issue of this journal, but has not been fully edited. Content may change prior to final publication. Citation information: DOI 10.1109/LRA.2021.3072855, IEEE Robotics and Automation Letters

TURCO *et al.*: GRASP PLANNING EXPLOITING EMBEDDED AND ENVIRONMENTAL CONSTRAINTS 5

TABLE II: Dataset of objects.

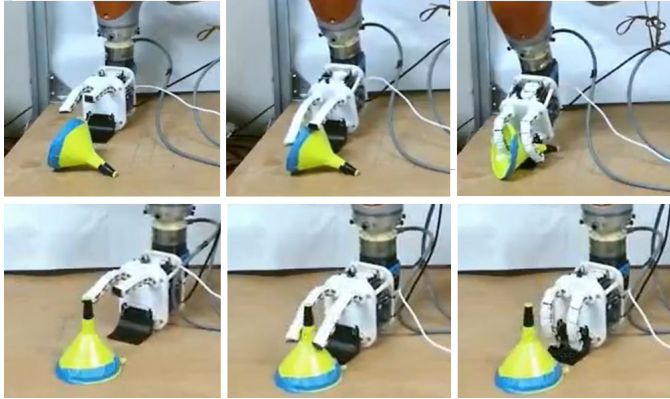| ID	Object	Weight (g)	Size (mm)
1	banana (YCB)	66	36×190
2	apple (YCB)	68	75
3	toy dolphin	84	$80 \times 200 \times 90$
4	spring clamp (YCB)	59	$90 \times 115 \times 27$
5	pasta pack	510	$65 \times 114 \times 182$
6	metal mug (YCB)	118	80×82
7	metal bowl (YCB)	147	159×53
8	cracker box (YCB)	411	$60 \times 158 \times 210$
9	gelatin box (YCB)	97	$28 \times 85 \times 73$
10	screwdriver (YCB)	98.4	31×215
11	chips can (YCB)	205	75×250
12	plastic funnel	21	125×115

Fig. 5: Experiment 1: grasp success (top) and failure (bottom) of the funnel.

A. Experiment 1: scoop grasp exploiting a table

First, we decided to analyze the case where the object is placed on a table, far from any other possible constraint. The scene segmentation algorithm recognizes that no walls or inclined planes are exploitable by the SSG. Then, the optimization problem is solved considering that the scoop will slide on the table and the constrained variables are referred to the reference frame placed on the table itself. The grasp is executed as explained in Sec. II-C and two trials (a success and a failure) are shown in Fig. 5. We carried out 110 trials with this setup, 10 for each object. The third column of Table III shows the obtained success rates.

TABLE III: Success rates obtained in Experiment 1 and in the two conditions tested in Experiment 2.

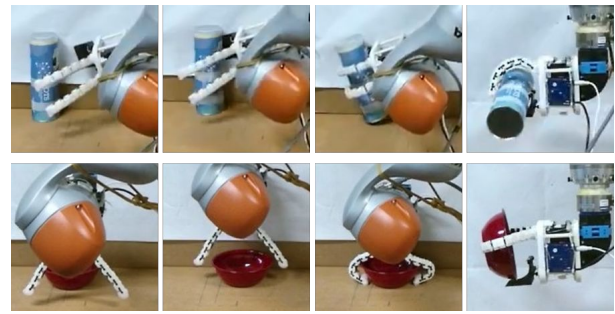| ID	Object	Exp. 1	Exp. 2 (wall)	Exp. 2 (table)
1	banana	10/10	3/6	5/6
2	apple	10/10	3/3	3/3
3	toy dolphin	10/10	6/6	6/6
4	spring clamp	9/10	8/18	16/18
5	pasta pack	4/10	7/18	12/18
6	metal mug	10/10	3/3	3/3
7	metal bowl	10/10	3/3	3/3
8	gelatin box	8/10	6/18	16/18
9	screwdriver	6/10	1/6	3/6
10	chips can	9/10	9/9	9/9
11	plastic funnel	8/10	7/9	9/9
	TOTAL	94/110	56/99	85/99

Fig. 6: Experiment 2: grasps from the wall: only the wall constraint is exploited (top); the scoop slides on the wall and the fingers slide on the table and grasp the object thanks to their compliance (bottom).

B. Experiment 2: scoop grasp exploiting a table or a wall

The second experiment consists in grasping objects which are constrained from two sides. The objects were placed close to a vertical wall and we tested two different types of grasp approaches: *i)* scoop sliding on the wall, towards the object, *ii)* scoop sliding on the table towards the object. In the first case, the optimization algorithm is solved considering that the sliding surface is vertical, thus, in the simulation, the hand is rotated to approach the object from above.

In both approaches, depending on the desired scoop orientation, the fingers might end up touching the constraint perpendicular to the exploited one, during their closure. To ensure a gentle slide and avoid a collapse of the fingers over the surface, we had to properly set the boundaries of the optimization variable d, based on the length of the fingers.

The two conditions were tested with the same 11 objects that were used in Experiment 1. Each object was placed in a certain orientation with respect to the environmental constraints, with one side touching the wall and one touching the table. Then it was grasped with the two different approaches. While in Experiment 1 we performed 10 trials for each object, in Experiment 2 we performed 3 trials for each possible object orientation with respect to the environmental constraints. Objects with a rounded shape (apple, mug, bowl), for example, were tested 3 times per strategy as they have only one possible orientation with respect to the wall, without considering them upside-down since the apple is almost spherical and for the other two objects we want to keep the hollow part up. The box, instead, as well as the pasta pack and the spring clamp were tested in 6 different orientations. Obtained results are summarized in the fourth and fifth columns of Table III. Successful trials obtained letting the scoop sliding on the wall and on the table are shown in Fig. 6 and in Fig. 7, respectively.

C. Experiment 3: use cases

Experiment 3 deals with use case scenarios. In particular, we analysed cases where the surface of an object is used to carry out a scoop grasp (Fig. 8a) and cases where the scoop is used inside a box (Fig. 8b). Two additional objects were used: a candy tube (18×228 mm, 12 g) and a box ($74 \times 153 \times 125$ mm, 93 g). A total of 9 experiments were performed
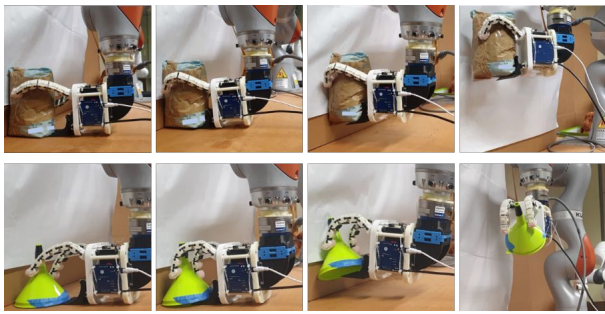
Fig. 7: Experiment 2. Successful grasp of the pasta pack (top) and of the funnel (bottom) exploiting the table.
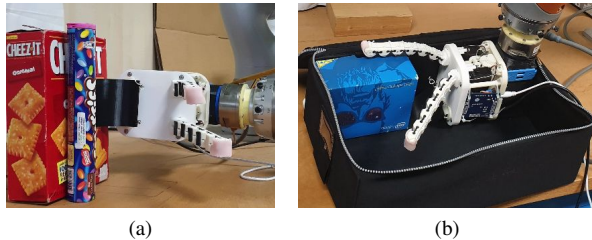

(a)   (b)

Fig. 8: Experiment 3. (a) Scoop grasp exploiting another object (cracker box). (b) Scoop grasp inside a box.

for each use case (6 for the box, and 3 for the candy tube), i.e., one test for each possible object orientation. In the first scenario, the surface of the cracker box was used as a sliding plane, and we obtained 8 successes out of 9 grasps. The second scenario involved grasping an object inside a box, exploiting also the internal walls as additional constraints. In this case, we achieved 7 successes out of 9 trials.

IV. DISCUSSION

Previously presented results indicate that the SSG can grasp a wide range of objects with the same strategy, exploiting hand reconfigurability, and embedded and environmental constraints. Considering all objects grasped with the configuration obtained with our optimization algorithm, 250 out of 326 grasps were successful, with an overall grasp success rate of about 77%. However, the conducted experiments are different in nature and need to be evaluated in detail.

A. Experiment 1: The scoop grasp strategy works well for different objects constrained only on one side.

The overall success rate of Experiment 1 is about 85%. This means that the adopted scoop grasp strategy works fine with different objects in different positions. In the following we will analyse in detail the relation between the success rate, the object features and the optimization variables.

In Fig. 9, we report a matrix of scatter plots and histograms of the data related to Experiment 1, which are gathered by dividing each variable into two groups: successful and unsuccessful grasps. Success rates are reported with respect to $\mathbf{x}$ and the objects' features. The selected properties are the object's weight and height; the second one is dependent on the object's pose.

As we can notice, in the first two histograms related to θ_R and θ_L, the workspace of the fingers is spanned in an unbalanced manner. Indeed, 76 out of 110 trials were performed exploiting ranges of the variables θ_R and θ_L belonging respectively to $[-21°, 0°]$ and $[0°, 21°]$. This is mainly related to the objects' height. Indeed, we can notice a correlation between the variation in height and the use of a certain range of θ_R and θ_L. Shorter objects are easily wrapped by caging the fingers towards the scoop, i.e., maintaining the two angles in a small interval near zero degrees. On the other hand, taller objects (such as chips can and pasta pack) are successfully grabbed by rotating the fingers in the ranges $[-120°, -50°]$ and $[50°, 120°]$ to push the object on the scoop towards the palm (see also Fig. 3).

In 56.4% of experiments, the optimization algorithm provided an object-hand distance d in the range $[0, 5]$ mm. These low values are mainly due to the effect of the second index introduced in the cost function, which tends to maximize the portion of the scoop area occupied by the object. No particular trends link the value of d to a failed grasp.

The variable γ, indicating the direction of the scoop approach towards the object, most of the times varies in the range $[-60°, 150°]$. The reason for this trend is related to the workspace of the robot arm. The failure trend is equally distributed across the range.

There are no remarkable trends for the variable α.

Lastly, as the weight increases, inevitably, the success rate will tend to zero once the payload value supported by the scoop is exceeded. In fact, 37.5% (6 out of 16) of failed grasps are related to the weight of the object (pasta pack).

B. Experiment 2: when the object is constrained on two sides, exploiting the table is most of the times more convenient than exploiting the wall.

In both the conditions tested within Experiment 2, the apple, the bowl, the metal mug, the chips can, and the toy dolphin were successfully grasped in all the orientations.

Short objects such as the banana, the gelatin box, and the screwdriver resulted difficult to be picked from the wall. This is mostly due to the fact that the SSG fingers are rather long and they need to be closed before reaching the object with the scoop to avoid their collapse over the table during the closure motion. A longer scoop (or shorter fingers) would avoid this problem. In general, a trade-off needs to be found. A longer scoop could facilitate the grasp from the wall, but, at the same time, might complicate the one from the table. The screwdriver was the object in the dataset picked up only once after sliding on the wall. The spring clamp was successfully grasped in almost half of the cases, and in two of these, the wall grasp succeeded, while the grasp from the table failed. Heavy objects like the pasta pack are very difficult to be picked up from the wall. One of the failed grasps of the pasta pack is shown in the top part of Fig. 10.

The grasp from the table failed only with the heavy pasta pack and with short objects (banana, gelatin box, spring clamp, screwdriver). The bottom part of Fig. 10 shows the failure obtained with the screwdriver: also here, like in the case of the
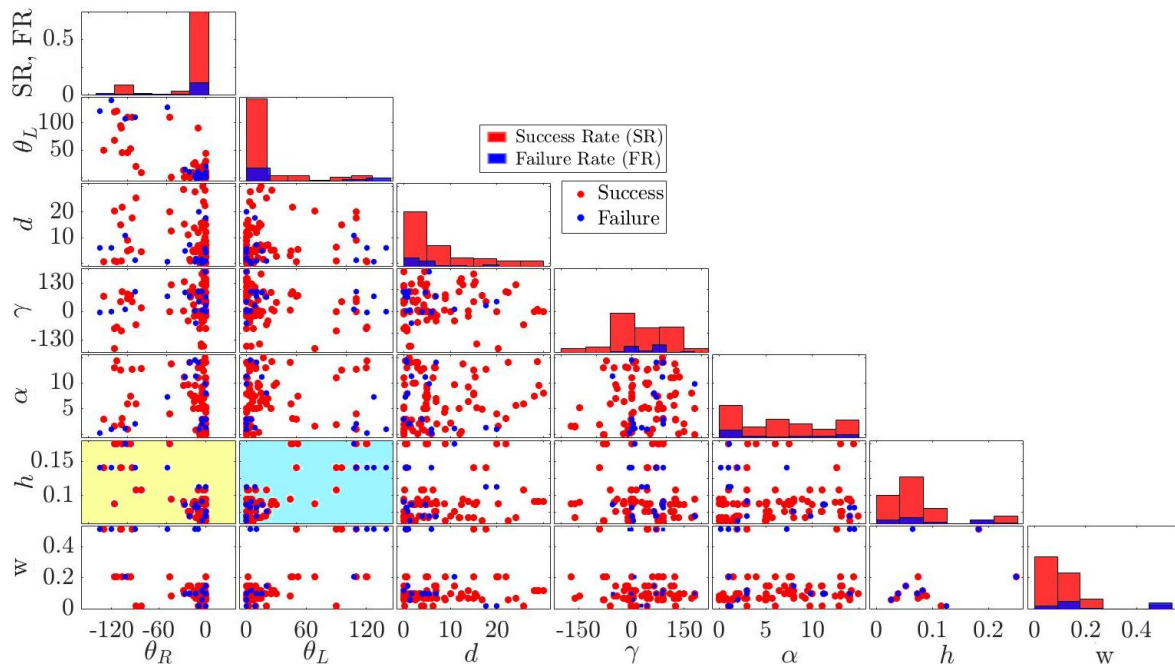
Fig. 9: Success and failure rates related to pre-grasp pose variables ($[\theta_R, \theta_L, d, \gamma, \alpha]$), and object characteristics (height h and weight w). Notice that the y-axis of the histograms reports the values of success and failures rates, going from 0 to 0.75 (see the y-axis label in the top left panel). All angles are expressed in degrees, the height in m and the weight in kg. The light yellow and light cyan boxes highlight the correlation between the orientations of the fingers (θ_R, θ_L) and the object height (h). The Pearson correlation coefficients $\rho_{\theta_R h}$, $\rho_{\theta_L h}$ are -0.82 and 0.79, respectively: the higher is the object, the greater are the absolute values of the angles.
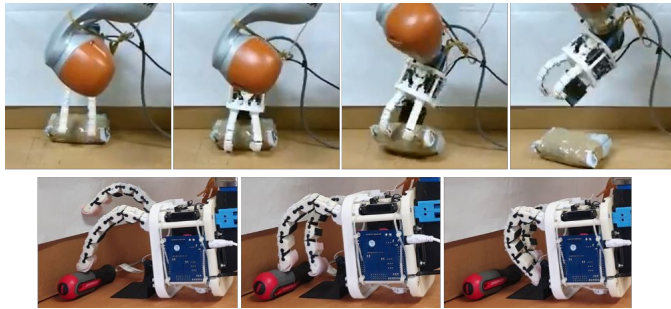

Fig. 10: Experiment 2: grasp failures. (top) Pasta pack reached from the wall. (bottom) Screwdriver from the table.

grasp from the wall, the fingers close before the scoop reaches the object. In general, the results of Experiment 2 show that when it is possible it is better to choose to grasp objects from the table (success rate: 86%) rather than from the wall (success rate: 56%). This is also due to the fact that while in the first case the scoop is perpendicular to the direction of the gravity, in the second, the weight of the object goes entirely on the fingers.

In contrast with Experiment 1, in which the hand grasps objects that are constrained only on one side, in Experiment 2 the second constraint can help to push the object on the scoop. This was shown to be particularly useful when the scoop slides on the table. Remarkable examples are the funnel and pasta pack (see Fig. 7). The first one was grasped in the only pose the gripper could not grasp it in Experiment 1 (Fig. 5). The

pasta pack was grasped 12 times out of 18, with a success rate of almost 67%, instead of 40%.

C. Experiment 3: the scoop grasp can be applied in real-world scenarios with constrained objects.

Experiment 3 had the objective of testing two possible applications of the scoop grasp. In the first, an object was used as a sliding surface to grab another one attached to it. This simulates a situation in which the object to grasp is so close to another that grasping it with classical grippers and strategies might be ineffective, unless using a very precise positioning of the gripper or using pushing motions to divide the objects. Thanks to the SSG we can use a single motion to achieve the grasp. Sliding between two objects, the scoop manages to separate them and grasp the object of interest while keeping the other in almost static conditions. In the 9 trials, there was only 1 failure, when the candy tube was put with the longest side attached to the cracker box. As discussed above, short objects are difficult to be picked from a surface perpendicular to the table.

In the second scenario, the object was placed inside a box, simulating a situation in which there are multiple environmental constraints. The task was to slide on the box bottom surface and grab objects by exploiting the box walls. In this case, also the corners can be used (object constrained from three sides). The exploitation of the additional surface is made possible by the reconfigurability of the fingers (see Fig. 8b), which allows avoiding collisions with the box wall. The grasp succeeded

in 7 out of 9 trials. The 2 failures were recorded with the candy tube. The first one was due to the box size that did not permit the hand to slide under the object. The second one was related to the box inclination that did not allow the candy tube to stand in a vertical position.

V. Conclusion and future work

In this paper, we presented an approach to grasp objects exploiting the embodied constraint (a scoop) and the reconfigurable fingers of a soft gripper. We implemented the so-called "scoop grasp", where the soft fingers are exploited to cage the object on the inherent constraint while it slides under the object itself.

Through the use of an optimization algorithm taking as input the point cloud of the object to be grasped, we searched for the best configuration of the fingers and the best pre-grasp pose for each object. We shaped the cost function of the optimization problem such that the grasp is robust and the embodied constraint is efficiently used. Even though the proposed algorithm is thought to be used with a particular gripper, the SSG, the general approach of combining two terms, one considering the grasp quality and one taking into account the actual exploitation of the embedded constraint, could also be applied to other similar devices.

We performed three different experiments over various objects. Experimental results show that reconfigurable soft grippers with embedded constraints represent a viable alternative to more complex soft hands if used with grasping strategies that allow exploiting their features. Reconfigurability allows grasping a variety of objects, whereas the use of the scoop allows exploiting the surfaces in contact with the objects. The intrinsic and passive adaptability of the hand is key to the success of the scoop grasp.

In future work, we will study whether a synergistic approach combining hand design and grasp planning can lead to improved success rates. We will investigate how to adapt the hand design (e.g., scoop length, joints stiffness, finger length, etc.) to the characteristics of the objects, possibly introducing variables related to the hand design in the optimization problem. Future research will also focus on the development of an algorithm able to determine on which plane the SSG should slide on based on the detected scene.

References

[1] R. Deimel, C. Eppner, J. Álvarez-Ruiz, M. Maertens, and O. Brock, "Exploitation of environmental constraints in human and robotic grasping," in *Robotics Research*. Springer, 2016, pp. 393–409.

[2] O. Brock, J. Park, and M. Toussaint, *Mobility and Manipulation*. Cham: Springer International Publishing, 2016, pp. 1007–1036. [Online]. Available: https://doi.org/10.1007/978-3-319-32552-1_40

[3] J. Bimbo, E. Turco, M. Ardahani, M. Pozzi, G. Salvietti, V. Bo, M. Malvezzi, and D.Prattichizzo, "Exploiting robot hand compliance and environmental constraints for edge grasps," *Frontiers in Robotics and AI*, no. 0, 2019.

[4] K. Hang, A. S. Morgan, and A. M. Dollar, "Pre-grasp sliding manipulation of thin objects using soft, compliant, or underactuated hands," *IEEE Robotics and Automation Letters*, vol. 4, no. 2, pp. 662–669, April 2019.

[5] G. Salvietti, Z. Iqbal, M. Malvezzi, T. Eslami, and D. Prattichizzo, "Soft hands with embodied constraints: The soft scoopgripper," in *Proc. IEEE Int. Conf. on Robotics and Automation*, Montreal, Canada, May 2019, pp. 2758–2764.

[6] C. Eppner and O. Brock, "Grasping unknown objects by exploiting shape adaptability and environmental constraints," *2013 IEEE/RSJ International Conference on Intelligent Robots and Systems*, 2013.

[7] K. Kosuge, J. Lee, J. Ichinose, and Y. Hirata, "A novel grasping mechanism for flat-shaped objects inspired by lateral grasp," in *2008 2nd IEEE RAS & EMBS International Conference on Biomedical Robotics and Biomechatronics*. IEEE, 2008, pp. 282–288.

[8] F. Levesque, B. Sauvet, P. Cardou, and C. Gosselin, "A model-based scooping grasp for the autonomous picking of unknown objects with a two-fingered gripper," *Robotics and Autonomous Systems*, vol. 106, pp. 14–25, 2018.

[9] M. Pozzi, S. Marullo, G. Salvietti, J. Bimbo, M. Malvezzi, and D. Prattichizzo, "Hand closure model for planning top grasps with soft robotic hands," *The International Journal of Robotics Research*, vol. 0, no. 0, 2020.

[10] C. Della Santina, V. Arapi, G. Averta, F. Damiani, G. Fiore, A. Settimi, M. G. Catalano, D. Bacciu, A. Bicchi, and M. Bianchi, "Learning from humans how to grasp: a data-driven architecture for autonomous grasping with anthropomorphic soft hands," *IEEE Robotics and Automation Letters*, vol. 4, no. 2, pp. 1533–1540, 2019.

[11] C. Gabellieri, F. Angelini, V. Arapi, A. Palleschi, M. G. Catalano, G. Grioli, L. Pallottino, A. Bicchi, M. Bianchi, and M. Garabini, "Grasp it like a pro: Grasp of unknown objects with robotic hands based on skilled human expertise," *IEEE Robotics and Automation Letters*, vol. 5, no. 2, pp. 2808–2815, 2020.

[12] C. Choi, W. Schwarting, J. DelPreto, and D. Rus, "Learning object grasping for soft robot hands," *IEEE Robotics and Automation Letters*, vol. 3, no. 3, pp. 2370–2377, 2018.

[13] A. M. Dollar and R. D. Howe, "The highly adaptive sdm hand: Design and performance evaluation," *The International Journal of Robotics Research*, vol. 29, no. 5, pp. 585–597, 2010. [Online]. Available: http://dx.doi.org/10.1177/0278364909360852

[14] J. Hughes, U. Culha, F. Giardina, F. Guenther, A. Rosendo, and F. Iida, "Soft manipulators and grippers: A review," *Frontiers in Robotics and AI*, vol. 3, p. 69, 2016. [Online]. Available: https://www.frontiersin.org/article/10.3389/frobt.2016.00069

[15] G. Salvietti, Z. Iqbal, I. Hussain, D. Prattichizzo, and M. Malvezzi, "The co-gripper: a wireless cooperative gripper for safe human robot interaction," in *Proc. IEEE/RSJ Int. Conf. Intelligent Robots and Systems*, Madrid, Spain, 2018, pp. 4576–4581.

[16] H.-C. Fu, J. D. Ho, K.-H. Lee, Y. C. Hu, S. K. Au, K.-J. Cho, K. Y. Sze, and K.-W. Kwok, "Interfacing soft and hard: a spring reinforced actuator," *Soft Robotics*, vol. 7, no. 1, pp. 44–58, 2020.

[17] Y. Tang, Y. Chi, J. Sun, T.-H. Huang, O. H. Maghsoudi, A. Spence, J. Zhao, H. Su, and J. Yin, "Leveraging elastic instabilities for amplified performance: Spine-inspired high-speed and high-force soft robots," *Science Advances*, vol. 6, no. 19, p. eaaz6912, 2020.

[18] L. Chin, F. Barscevicius, J. Lipton, and D. Rus, "Multiplexed manipulation: Versatile multimodal grasping via a hybrid soft gripper," in *2020 IEEE International Conference on Robotics and Automation (ICRA)*. IEEE, 2020, pp. 8949–8955.

[19] D. Prattichizzo and J. C. Trinkle, "Grasping," in *Springer handbook of robotics*, B. Siciliano and O. Khatib, Eds. Springer Science & Business Media, 2016, pp. 955–988.

[20] M. A. Roa and R. Suarez, "Grasp quality measures: review and performance," *Autonomous Robots*, vol. 38, no. 1, pp. 65–88, 2015.

[21] C. R. Houck, J. Joines, and M. G. Kay, "A genetic algorithm for function optimization: a matlab implementation," *Ncsu-ie tr*, vol. 95, no. 09, pp. 1–10, 1995.

[22] M. Malvezzi, G. Gioioso, G. Salvietti, and D. Prattichizzo, "Syngrasp: A matlab toolbox for underactuated and compliant hands," *IEEE Robotics & Automation Magazine*, vol. 22, no. 4, pp. 52–68, 2015.

[23] X.-S. Yang, "Nature-inspired optimization algorithms: Challenges and open problems," *Journal of Computational Science*, vol. 46, p. 101104.

[24] R. c. Willow Garage, "ORK Object Recognition Kitchen," https://github.com/wg-perception/object_recognition_core.

[25] R. B. Rusu and S. Cousins, "3D is here: Point Cloud Library (PCL)," in *IEEE International Conference on Robotics and Automation (ICRA)*, Shanghai, China, May 9-13 2011.

[26] N. Amenta, M. Bern, and M. Kamvysselis, "A new voronoi-based surface reconstruction algorithm," in *Proceedings of the 25th annual conference on Computer graphics and interactive techniques*, 1998, pp. 415–421.

[27] B. Calli, A. Walsman, A. Singh, S. Srinivasa, P. Abbeel, and A. M. Dollar, "Benchmarking in manipulation research: Using the yale-cmu-berkeley object and model set," *Robot. Automat. Mag.*, vol. 22, 2015.